Local Thermal Non-equilibrium in Porous Medium Convection

D.A.S.Rees[1] & I. Pop[2]

[1]Department of Mechanical Engineering, University of Bath, Bath BA2 7AY, U.K.
[2]Faculty of Mathematics, University of Cluj, Cluj, Romania

KEYWORDS

Local thermal non-equilibrium, convection, porous media.

ABSTRACT

Many papers exist which either derive or use equations which govern local thermal nonequilibrium phenomena in porous medium convection, where the intrinsic average of the temperatures of the solid and fluid phases may be regarded as being different. We compile and present the most commonly used of these model equations. Attention is then focused on describing some of the most recent research using these equations. Attention is focussed primarily on free and forced covection boundary layers, and on free convection within cavities.

INTRODUCTION

In this chapter we consider the subject of Local Thermal NonEquilibrium, LTNE. In most cases studied in the research literature it has been assumed that a porous matrix and the fluid which flows through it are in Local Thermal Equilibrium, LTE. At a microscopic level, the temperature and the rate of heat flux at the interface between the solid and fluid phases must be identical, but the average temperature over a Representative Elementary Volume, REV, does not have to yield identical temperatures for the two phases. For instance, one may consider the example of a hot highly conducting fluid flowing through an otherwise cold and poorly conducting porous matrix; in this case a certain amount of time will need to pass before the solid phase attains the same temperature as the fluid phase. We will also see that LTNE is not necessarily an unsteady phenomenon, but can also arise in steady flows. An example of this would be a case where cold poorly conducting fluid is drawn by suction towards a hot permeable surface — in this case the resulting steady thermal boundary layer within the solid phase extends further from the hot surface than it does in the fluid phase.

One aim of this chapter is to introduce briefly those equations which have been quoted as

modelling LTNE effects in porous media. We have found that it is only the simplest of these model equations which have been routinely solved for specific convective flows. The second aim is to summarise the most recent studies of applications, which are primarily in the area of free convection and external forced convection. An excellent review of all but the very latest studies of internal forced convection cases may be found in Kuznetsov (1998). We do not attempt to present the derivations of the thermal energy equations which apply when LTNE is present; instead we refer the reader to the book by Whitaker (1999), the chapters by Carbonell and Whitaker (1984), Quintard *et al.* (1997) and Quintard and Whitaker (2000) and the paper by Quintard (1998). An excellent review of conductive effects in a stagnant porous medium may be found in Cheng and Hsu (1998).

The Chapter is organised as follows. We begin with a summary of the governing equations which are currently available to study either conduction or convection within a porous medium using the two-temperature model. This is followed by a brief discussion of general indications of when the one-temperature model may or may not be used. The remaining sections are concerned with free convection boundary layer flows, recent forced convection studies and problems in stability theory, respectively.

GOVERNING EQUATIONS

Nield and Bejan (1999) quote the following equations as the simplest way in which LTNE may be modelled:

$$\epsilon(\rho c)_{\rm f}\frac{\partial T_{\rm f}}{\partial t} + (\rho c)_{\rm f}\underline{v}.\nabla T_{\rm f} = \epsilon\nabla.(k_{\rm f}\nabla T_{\rm f}) + h(T_{\rm s} - T_{\rm f}), \tag{1}$$

$$(1-\epsilon)(\rho c)_{\rm s}\frac{\partial T_{\rm s}}{\partial t} = (1-\epsilon)\nabla.(k_{\rm s}\nabla T_{\rm s}) + h(T_{\rm f} - T_{\rm s}). \tag{2}$$

This is sometimes called the two-temperature model. In these equations ϵ is the porosity of the porous medium, the subscripts f and s denote fluid and solid properties, respectively, while other variables take their familiar meanings. The variable h is an inter-phase heat transfer coefficient. In eqs. (1) and (2) we follow the standard practice that $T_{\rm f}$ and $T_{\rm s}$ are intrinsic averages of the temperature fields, and this allows us to set $T_{\rm f} = T_{\rm s} = T_0$ whenever the boundary of the porous medium is maintained at the temperature T_0. On the other hand, $\underline{v}$ is a superficial average; see Quintard and Whitaker (2000, p5).

Equations similar in form to (1) and (2) but without the diffusion terms were derived by Schumann (1929) using a straightforward control volume technique. This is the first known author to consider separately the temperature fields of the solid and the fluid phases.

When $T_{\rm s} > T_{\rm f}$ the final term in eq. (1) acts as a source of thermal energy into the fluid phase, while the final term in eq. (2) is a thermal sink for the solid phase. Eq. (1) also shows us that, when a medium is of low porosity ($\epsilon \ll 1$) and the solid and fluid phases exhibit the temperature difference, ΔT, then the rate of change of the fluid temperature is $O(h\Delta T/\epsilon(\rho c)_{\rm f})$. As this is inversely proportional to ϵ, there is a rapid change in the fluid temperature towards that of the solid phase in order to establish LTE.

When LTE applies, then $T_{\rm f} = T_{\rm s}$ everywhere, and the equations may be combined by addition to yield the one-temperature model,

$$(\rho c)_{\rm eff}\frac{\partial T}{\partial t} + (\rho c)_{\rm f}\underline{v}.\nabla T = \nabla.(k_{\rm eff}\nabla T), \tag{3}$$

where the effective porous medium properties are given by

$$(\rho c)_{\rm eff} = \epsilon(\rho c)_{\rm f} + (1-\epsilon)(\rho c)_{\rm s}, \tag{4}$$

$$k_{\rm eff} = \epsilon k_{\rm f} + (1-\epsilon)k_{\rm s}. \tag{5}$$

Expression (5) is almost always quoted as being the definition of the effective conductivity of the saturated porous medium, where T may now be regarded as a superficial average. However, Nield (2002) points out that expression (5) corresponds to thermal resistances in series such as one would have when considering heat conduction in the direction parallel to alternating layers of fluid and solid. When conduction takes place perpendicular to such interfaces, then he suggests the following definition of $k_{\rm eff}$,

$$\frac{1}{k_{\rm eff}} = \frac{\epsilon}{k_{\rm f}} + \frac{1-\epsilon}{k_{\rm s}}. \tag{6}$$

Thus, for a layered medium, such as is given by a parallel plate channel, the effective conductivities are different in the two main directions. Nield concludes that, for such a structured medium where the fluid/solid interfaces are parallel with the x-direction, the appropriate LTNE equations to be used are given by,

$$\epsilon(\rho c)_{\rm f}\frac{\partial T_{\rm f}}{\partial t} + (\rho c)_{\rm f}\underline{v}.\nabla T_{\rm f} = \epsilon\Big[\frac{\partial}{\partial x}\Big(k'_{\rm f}\frac{\partial T_{\rm f}}{\partial x}\Big) + \frac{\partial}{\partial y}\Big(k_{\rm f}\frac{\partial T_{\rm f}}{\partial y}\Big)\Big] + h(T_{\rm s}-T_{\rm f}), \tag{7}$$

$$(1-\epsilon)(\rho c)_{\rm s}\frac{\partial T_{\rm s}}{\partial t} = (1-\epsilon)\Big[\frac{\partial}{\partial x}\Big(k'_{\rm s}\frac{\partial T_{\rm s}}{\partial x}\Big) + \frac{\partial}{\partial y}\Big(k_{\rm s}\frac{\partial T_{\rm s}}{\partial y}\Big)\Big] + h(T_{\rm f}-T_{\rm s}), \tag{8}$$

where

$$k'_{\rm f} = k'_{\rm s} = \frac{k_{\rm f}k_{\rm s}}{\epsilon k_{\rm s} + (1-\epsilon)k_{\rm f}}. \tag{9}$$

At the time of writing only one paper has considered Nield's model; see Kim and Kuznetsov (2003).

More complex models than those given above have been proposed. Alazmi and Vafai (2000) have undertaken a comprehensive series of numerical experiments using a forced convection channel flow to determine whether the different expressions used for the various coefficients used in equations for convective flows in porous media give rise to significant differences in the solutions of those equations. This was a general study which, in addition to LTNE effects, also considered the Forchheimer and Brinkman terms and different models for both porosity and thermal dispersion. Focussing here on the LTNE between the phases, Alazmi and Vafai (2000) use the following equations for the steady-state two-temperature model,

$$(\rho c)_{\rm f}\underline{v}.\nabla T_{\rm f} = \nabla.(k_{\rm f\,eff}.\nabla T_{\rm f}) + h_{\rm sf}a_{\rm sf}(T_{\rm s}-T_{\rm f}), \tag{10}$$

$$0 = \nabla.(k_{\rm s\,eff}.\nabla T_{\rm s}) - h_{\rm sf}a_{\rm sf}(T_{\rm s}-T_{\rm f}). \tag{11}$$

In these equations

$$k_{\rm f\,eff} = \epsilon k_{\rm f}, \qquad \text{and} \qquad k_{\rm s\,eff} = (1-\epsilon)k_{\rm s}, \tag{12}$$

are regarded as tensor quantities, but the diffusion terms reduce to those given in eqs. (1) and (2) when $k_{\rm f}$ and $k_{\rm s}$ are constants. The value h given in eqs. (1) and (2) has now been replaced by the product of $h_{\rm sf}$ and $a_{\rm sf}$, where the former is the heat-to-fluid heat transfer coefficient and the

latter is the specific surface area of the solid phase. Three different combinations of expressions for these coefficients were considered by Alazmi and Vafai (2000). Case E1 is given by

$$h_{\rm sf} = \frac{k_{\rm f}(2 + 1.1{\rm Pr}^{1/3}{\rm Re}^{0.6})}{d_p}, \qquad a_{\rm sf} = \frac{6(1-\epsilon)}{d_p}, \tag{13}$$

where the expression for $h_{\rm sf}$ is an experimental correlation obtained by Wakao *et al.* (1979), and that for $a_{\rm sf}$ may be found in Dullien (1979). Case E2 is

$$h_{\rm sf} = 0.004\Big(\frac{d_{\rm Nu}}{d_p}\Big)\Big(\frac{k_{\rm f}}{d_p}\Big){\rm Pr}^{0.33}{\rm Re}^{1.35} \quad ({\rm Re} < 75),$$

$$h_{\rm sf} = 1.064\Big(\frac{k_{\rm f}}{d_p}\Big){\rm Pr}^{0.33}{\rm Re}^{0.59} \quad ({\rm Re} > 350), \tag{14a}$$

$$a_{\rm sf} = \frac{20.346(1-\epsilon)\epsilon^2}{d_p}, \tag{14b}$$

which may be found in Hwang *et al.* (1995). We note that no information is given there about the intermediate regime where $75 < {\rm Re} < 350$. Finally case E3 is

$$\Big[\frac{d_p\epsilon}{0.2555{\rm Pr}^{1/3}{\rm Re}^{2/3}k_{\rm f}} + \frac{d_p}{10k_{\rm s}}\Big]^{-1}, \qquad a_{\rm sf} = \frac{6(1-\epsilon)}{d_p}, \tag{15}$$

where the expression for $h_{\rm sf}$ was derived by Dixon and Cresswell (1979). In the above expressions, d_p is the particle diameter, $d_{\rm Nu} = 4\epsilon/a_{\rm sf}$, see Alazmi and Vafai (2000), ${\rm Pr} = \mu C_{\rm f}/k_{\rm f}$ is the Prandtl number, and ${\rm Re} = uL/{\rm Nu}$ is the Reynolds number which is based on the macroscopic lengthscale, L.

The conclusions of the comparative study by Alazmi and Vafai (2000) are very detailed, but they find that the three models give close results when the porosity is high, or when Re is large or when the particle diameters are small.

The paper by Kuwahara *et al.* (2001) reports on a fully numerical simulation of the flow and heat transfer through a periodic array of square cylinders. The aim of the numerical study was to find a correlation for $h_{\rm sf}$ as a function of the microscopic Reynolds number, the Prandtl number and the porosity. Using the present notation, it was found that

$$h_{\rm sf} = \frac{k_{\rm f}}{d_p}\Big[\Big(1 + \frac{4(1-\epsilon)}{\epsilon}\Big) + \frac{1}{2}(1-\epsilon)^{1/2}{\rm Re}^{0.6}{\rm Pr}^{1/3}\Big]. \tag{16}$$

A slightly earlier study by Amiri and Vafai (1998) had similar aims to those of Alazmi and Vafai (2000) but concentrated on the transient development of the temperature fields. In this earlier paper the authors used the Case E1 expressions above, and the following expressions for the thermal conductivities in the x and y-directions,

$$k_{{\rm f\,eff}\,x} = k_{\rm f}\Big[\epsilon + 0.5\Big(\frac{\rho_{\rm f}\,u\,d_p}{\mu_{\rm f}}\Big){\rm Pr}\Big], \tag{17}$$

$$k_{{\rm f,\,eff}\,y} = k_{\rm f}\Big[\epsilon + 0.1\Big(\frac{\rho_{\rm f}\,u\,d_p}{\mu_{\rm f}}\Big){\rm Pr}\Big], \tag{18}$$

which were obtained from Wakao and Kaguei (1982). These two coefficients play the same role as do $\epsilon k_{\rm f}'$ and $\epsilon k_{\rm f}$ in eq. (7). The first terms on the right hand sides of expressions (17) and (18) are the stagnant conductivities, while the second terms are the dispersion conductivities based on uniform flow in the x-direction. It is frequently the case that these dispersion conductivities are neglected. Other forms for the dispersion coefficients are quoted by Vafai and Amiri (1998).

Recently, Fourie and Du Plessis (2003a) have derived the following version of the two-temperature model for conduction only:

$$\epsilon(\rho c)_{\rm f}\frac{\partial T_{\rm f}}{\partial t} = \nabla.(k_{\rm ff}\nabla T_{\rm f}) + \nabla.(k_{\rm fs}\nabla T_{\rm s}) + a_{\rm sf}h_{\rm sf}(T_{\rm s} - T_{\rm f}), \tag{19}$$

$$(1-\epsilon)(\rho c)_{\rm s}\frac{\partial T_{\rm s}}{\partial t} = \nabla.(k_{\rm ss}\nabla T_{\rm s}) + \nabla.(k_{\rm sf}\nabla T_{\rm f}) + a_{\rm sf}h_{\rm sf}(T_{\rm f} - T_{\rm s}), \tag{20}$$

where we have omitted volumetric heat source terms, and where we have translated their notation from superficial to intrinsic variables. In these equations the quantities, $k_{\rm ff}$ and $k_{\rm fs}$ are called the fluid phase effective thermal conductivity tensor and the fluid phase coupled thermal conductivity tensor, respectively. Likewise, $k_{\rm ss}$ and $k_{\rm sf}$ are called the solid phase effective thermal conductivity tensor and the solid phase coupled thermal conductivity tensor, respectively. Although this model has appeared in earlier works, such as that of Quintard and Whitaker (1993), Fourie and Du Plessis (2003a) gave a formula for the conductivity tensors which may be evaluated for certain classes of porous media, as illustrated in Fourie and Du Plessis (2003b). Quintard and Whitaker (1993) also showed that $k_{\rm sf} = k_{\rm fs}$. An extension of eqs. (19) and (20) to convective flows has also been derived by Carbonell and Whitaker (1984) and used by Zhang and Huang (2001) for the developing thermal field in a porous channel, with additional comments by Magyari and Keller (2002) and Zhang and Huang (2002).

Finally, it is necessary to consider briefly the subject of boundary conditions. For the case where a fixed temperature is imposed upon the boundary of a porous domain, then the appropriate boundary conditions which are generally used correspond to LTE locally, i.e. one sets $T_{\rm f} = T_{\rm s} = T_0$ on the boundary. If the bounding surface is located at $x = 0$, the local rate of heat transfer may then be written as

$$q_w'' = -\left[\epsilon k_{\rm f}\frac{\partial T_{\rm f}}{\partial x} - (1-\epsilon)k_{\rm s}\frac{\partial T_{\rm s}}{\partial x}\right]_{x=0}. \tag{21}$$

Thus a global Nusselt number may be defined in the usual way, although it is frequently the case that separate Nusselt numbers for the two phases are presented. However, when a uniform heat flux boundary condition is to be imposed, then the situation is not so straightforward. Kim and Kim (2001) considered the relative merits of two different approaches to this situation which were originally proposed by Amiri *et al.* (1994). In the First Approach the imposed heat flux is split between the phases according to eq. (21) where q_w'' is now interpreted as being the imposed heat flux. In view of the fact that two second order thermal energy equations are being solved, (21) is then supplemented by the LTE condition $T_{\rm f} = T_{\rm s}$ on the surface. In the Second Approach it is assumed that the heat flux into the two phases are the same, i.e.

$$q'' = -\epsilon k_{\rm f}\frac{\partial T_{\rm f}}{\partial x}\bigg|_{x=0} = (1-\epsilon)k_{\rm s}\frac{\partial T_{\rm s}}{\partial x}\bigg|_{x=0}. \tag{22}$$

Equation (22) represents two boundary conditions, and therefore the temperatures of each phase must be found as part of the final solution. Kim and Kim (2001) consider two different practical situations involving forced convective flow and conclude that the First Approach is

to be preferred in general. However, they make an important caveat that the thickness of the impermeable boundary is significant. When it is sufficiently thick compared with the microscopic lengthscale, which is a typical practical situation, then the First Approach is applicable. Otherwise, when it is thin or nonexistent, the Second Approach must be used.

CONDITIONS FOR THE VALIDITY OF LTE

Most papers which deal with convective flows in porous media assume that LTE is valid, and it is therefore important to acquire some criteria which will indicate when this is not a good assumption.

Nield (1998), using eqs. (1) and (2), considered steady conduction in a porous medium subject to an imposed temperature on the boundary of the domain, and where the conductivities of the phases are uniform. He showed that $T_\mathrm{f} = T_\mathrm{s}$ in this case by deriving a Helmholtz equation for $T_\mathrm{f} - T_\mathrm{s}$ which is subject to $T_\mathrm{f} - T_\mathrm{s} = 0$ on the boundary. Thus LTE always occurs in steady conduction problems where the boundary temperature is imposed. Then the implication is that any departure from this special state will give rise to LTNE in general, although cases where LTE pertains may always be derived as special cases.

The present authors have, in an incomplete and as yet unpublished study, considered unsteady conduction where the plane boundary of a semi-infinite porous medium has its temperature raised suddenly. If one were to assume LTE, then the resulting temperature field may be described using the complementary error function. When LTNE is assumed, the thermal fields in the two phases at early times correspond to complementary error functions with different arguments, and therefore strong LNTE effects are observed. However, as time progresses, the thermal front slows down, as its speed is inversely proportional to $t^{1/2}$, and LTE is eventually established. In this case rapid changes in boundary conditions result in LTNE.

Al-Nimr and Abu-Hijleh (2002) studied a channel flow problem using the equations of Schumann (1929), i.e. eqs. (1) and (2) without diffusion. At $t = 0$ the inlet temperature was raised suddenly and the authors investigated the subsequent change in the temperature field. At long times the problem becomes like that of Nield (1998) which is described at the beginning of this section, and therefore LTE is always achieved eventually. Therefore attention is focussed on the thermal relaxation time over which LTNE gives way to LTE. The final conclusions are lengthy, but it is found that the relaxation time is inversely proportional to the volumetric Biot number defined according to,

$$\mathrm{Bi} = \frac{hL}{(\rho c)_\mathrm{f} U}, \tag{23}$$

where U is the fluid velocity along the channel and L its length. Given the absence of diffusion, it is not surprising that the relaxation time is proportional to the imposed velocity.

Similar conclusions with regard to the rapidity of changing conditions have been made by Minkowycz *et al.* (1999) and Al-Nimr and Kiwan (2002), although the concern of each of these authors was with the effect of oscillating boundary conditions. Minkowycz *et al.* (1999) considered the effect of a suddenly imposed sinusoidally varying heat flux on the lower surface of a channel. When treated as a conduction problem only, it was found that LTE is valid in general when the Sparrow number satisfies, $\mathrm{Sp} > 100$. In terms of the present notation, the

Sparrow number is defined as

$$\mathrm{Sp} = \frac{h_{\mathrm{sf}} a_{\mathrm{sf}} L^2}{k}, \tag{24}$$

where L is the height of the channel and k the conductivity of the porous medium. When an imposed flow field is present then LTE is valid when $\mathrm{Sp/Pe} > 100$.

Al-Nimr and Kiwan (2002) also used Schumann's (1929) diffusion-free model to study the effect of a sinusoidally oscillating inlet temperature to a porous channel. The criterion for the validity of assuming LTE was based on the absence of a phase lag between the solid and fluid phases and is given by

$$\frac{h}{\bar{\omega}(\rho c)_{\mathrm{s}}(1-\epsilon)} > 20, \tag{25}$$

where $\bar{\omega}$ is the dimensional frequency of the inlet temperature. Again, we have translated the published criterion into the present notation.

It is clear that the papers by Minkowycz *et al.* (1999) and Al-Nimr and Kiwan (2002) yield different results since only the latter uses the oscillation frequency. However, these are not necessarily contradictory for they were obtained for somewhat different configurations.

FREE CONVECTION BOUNDARY LAYERS

General formulation

We consider the steady free convection around a two-dimensional symmetric body which is embedded in a fluid-saturated porous medium. It is assumed that the surface of the body is held at the constant temperature T_w, while the ambient temperature is T_∞, where $T_w > T_\infty$. If we assume that Darcy's law holds, that the Boussinesq approximation is valid, but that the LTE assumption does not apply, then the equations governing the two-temperature free convection flow model can be written in non-dimensional form as, see Rees and Pop (1999),

$$\frac{\partial \hat{u}}{\partial \hat{x}} + \frac{\partial \hat{v}}{\partial \hat{y}} = 0, \tag{26}$$

$$\frac{\partial \hat{u}}{\partial \hat{y}} - \frac{\partial \hat{v}}{\partial \hat{x}} = Ra \frac{\partial \theta}{\partial \hat{y}} S(\hat{x}), \tag{27}$$

$$\hat{u}\frac{\partial \theta}{\partial \hat{x}} + \hat{v}\frac{\partial \theta}{\partial \hat{y}} = \nabla^2 \theta + \hat{h}(\theta - \phi), \tag{28}$$

$$\nabla^2 \phi - \hat{h}\gamma(\theta - \phi) = 0, \tag{29}$$

where the nondimensional variables are defined as

$$(\overline{x}, \overline{y}) = d(\hat{x}, \hat{y}), \quad (\overline{u}, \overline{v}) = \frac{k_{\mathrm{f}}}{(\rho C_p)_{\mathrm{f}} d}(\hat{u}, \hat{v}),$$

$$T_{\mathrm{f}} = (T_w - T_\infty)\theta + T_\infty, \quad T_{\mathrm{s}} = (T_w - T_\infty)\phi + T_\infty. \tag{30}$$

Here $\overline{x}$ is the dimensional Cartesian coordinate which measures the distance from either the forward stagnation point along the surface of the symmetrical body or the leading edge, and $\overline{y}$ is in the normal direction. In addition the respective velocities are $\overline{u}$ and $\overline{v}$, T is the temperature.

and d is a suitably defined macroscopic lengthscale. The quantity $S(\hat{x})$ depends on the shape of the heated surface with $S(\hat{x}) = 1$ corresponding to a vertical surface and $S(\hat{x}) = \hat{x}$ to a stagnation point flow such as on the underside of a hot circular cylinder. Further, $\hat{h}$ and γ are dimensionless constants and Ra is the Darcy-Rayleigh number, which are defined as

$$\hat{h} = hd^2/\epsilon k_{\rm f}, \quad \gamma = \epsilon k_{\rm f}/(1-\epsilon)k_{\rm s}, \qquad Ra = (\rho C_p)_{\rm f} g K \beta (T_w - T_\infty)/\mu k_{\rm f}. \tag{31}$$

We introduce now a stream function $\hat{\psi}$ according to $\hat{u} = \partial\hat{\psi}/\partial\hat{y}$ and $\hat{v} = -\partial\hat{\psi}/\partial x$. Equations (26)-(29) thus become

$$\nabla^2\hat{\psi} = Ra\frac{\partial\theta}{\partial\hat{y}}S(\hat{x}), \tag{32}$$

$$\nabla^2\theta + \hat{h}(\phi - \theta) = \frac{\partial\hat{\psi}}{\partial\hat{y}}\frac{\partial\theta}{\partial\hat{x}} - \frac{\partial\hat{\psi}}{\partial\hat{x}}\frac{\partial\theta}{\partial\hat{y}}, \tag{33}$$

$$\nabla^2\phi + \hat{h}\gamma(\theta - \phi) = 0. \tag{34}$$

Let us now introduce the usual boundary-layer variables,

$$x = \hat{x}, \quad y = Ra^{1/2}\hat{y}, \quad \psi = Ra^{-1/2}\hat{\psi}, \tag{35}$$

into Eqs. (32)-(34) to obtain

$$\frac{\partial^2\psi}{\partial y^2} = \frac{\partial\theta}{\partial y}S(x), \tag{36}$$

$$\frac{\partial^2\theta}{\partial y^2} + H(\phi - \theta) = \frac{\partial\psi}{\partial y}\frac{\partial\theta}{\partial x} - \frac{\partial\psi}{\partial x}\frac{\partial\theta}{\partial y}, \tag{37}$$

$$\frac{\partial^2\phi}{\partial y^2} + H\gamma(\theta - \phi) = 0, \tag{38}$$

where we have omitted terms which are asymptotically small, compared with the retained terms as $Ra \to \infty$. In Eqs. (37) and (38) the dimensionless constant H is defined as

$$\hat{h} = Ra\, H, \tag{39}$$

where $H = O(1)$ as $Ra \to \infty$, allows the detailed study of how the boundary-layer undergoes the transition from strong thermal nonequilibrium near the body's leading edge to thermal equilibrium far from the leading edge. The boundary conditions of Eqs. (36)-(38) are give by

$$\psi = 0, \quad \theta = 1, \quad \phi = 1 \text{ at } y = 0, \quad x > 0, \tag{40a}$$

$$\frac{\partial\psi}{\partial y} \to 0, \ \theta \to 0, \ \phi \to 0 \text{ as } y \to \infty, \ x > 0 \tag{40b}$$

These boundary conditions allow Eq. (36) to be integrated once to yield

$$\frac{\partial\psi}{\partial y} = \theta S(x). \tag{41}$$

The physical quantities of most interest are the fluid and solid phase Nusselt numbers, which are defined as

$$\mathrm{Nu}_{\rm f} = \frac{Lq_{\rm f}}{k_{\rm f}(T_w - T_\infty)}, \quad \mathrm{Nu}_{\rm s} = \frac{Lq_{\rm s}}{k_{\rm s}(T_w - T_\infty)}, \tag{42}$$

where $q_{\rm f} = -k_{\rm f}(\partial T_{\rm f}/\partial\overline{y})_{\overline{y}=0}$ and $q_{\rm s} = -k_{\rm s}(\partial T_{\rm s}/\partial\overline{y})_{\overline{y}=0}$. Substituting variables (30) and (35) into expression (42), we obtain

$$\mathrm{Nu}_{\rm f}/Ra^{1/2} = -\left(\frac{\partial\theta}{\partial y}\right)_{y=0}, \qquad \mathrm{Nu}_{\rm s}/Ra^{1/2} = -\left(\frac{\partial\phi}{\partial y}\right)_{y=0}. \tag{43}$$

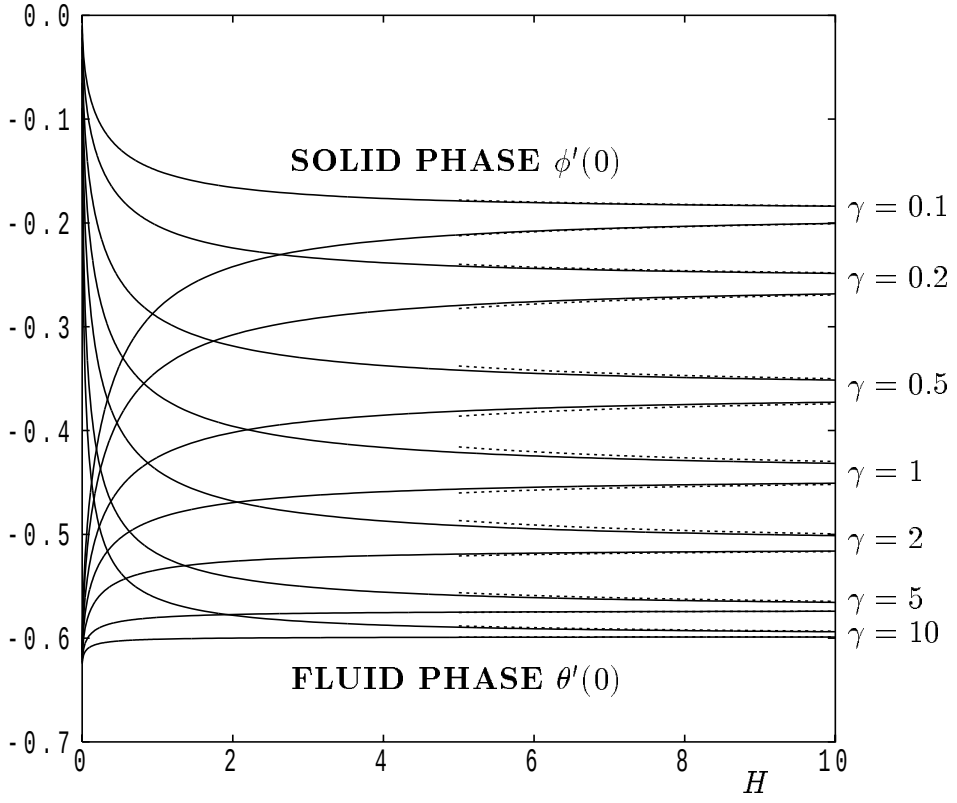

Figure 1: The variation of $\theta'(0)$ and $\phi'(0)$ with H for selected values of γ, as obtained by solving eqs. (46). The dotted lines correspond to the large-H asymptotic values given in expression (48).

Results for stagnation point flow

For stagnation-point flow we take

$$S(x) = x, \tag{44}$$

and write

$$\psi = xf(y), \quad \theta = \theta(y), \quad \phi = \phi(y). \tag{45}$$

Substituting expressions (44) and (45) into Eqs. (37), (38) and (41) leads to the following set of ordinary differential equations,

$$f' = \theta, \quad \theta'' + f\theta' = H(\theta - \phi), \quad \phi'' = H\gamma(\phi - \theta), \tag{46}$$

and the boundary conditions (40) become

$$f(0) = 0, \quad \theta(0) = 1, \quad \phi(0) = 1, \qquad \theta(\infty) = 0, \quad \phi(\infty) = 0, \tag{47}$$

where primes denote differentiation with respect to y.

The ordinary differential eqs. (46), subject to the boundary conditions (47), with H and γ as parameters were integrated numerically by Rees and Pop (1999) using the Keller-box method. The numerical results are summarized in Fig. 1 where $\theta'(0)$ and $\phi'(0)$ are represented for some values of H and γ. It is seen that when H is small, there is a very substantial difference between the surface rates of heat transfer of the fluid and solid phases, indicating that LTNE

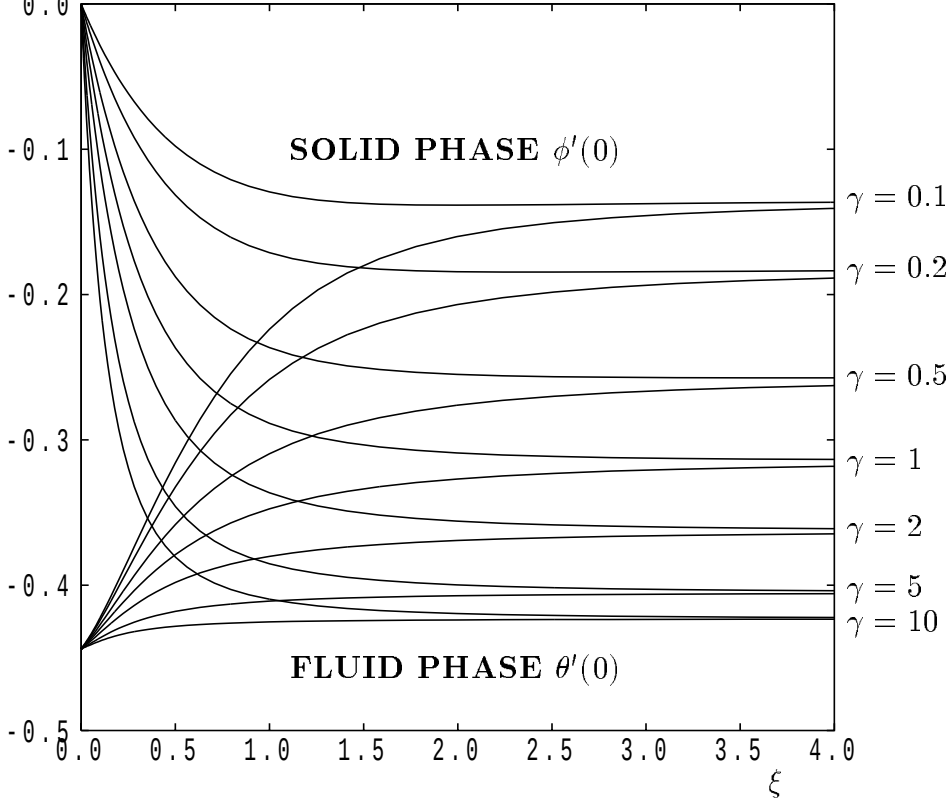

Figure 2: The variation of $\theta'(0)$ and $\phi'(0)$ with $\xi = (Hx)^{1/2}$ for selected values of γ, as obtained by solving eqs. (51) to (53).

effects are stronger when H is small, which is not surprising since H is a measure of the ease with which heat is transferred between the phases. As H increases, the inter-phase local heat transfer becomes more effective and this means that the difference between the solid and fluid temperature fields also decreases in magnitude and LTE is recovered. Fig. 1 also shows that the same qualitative effects are obtained as γ decreases.

Rees and Pop (1999) have also obtained asymptotic solutions of Eqs. (46) for large and, respectively, small values of the parameter H. Thus, it is shown that for large values of $H(\gg 1)$, the surface rates of heat transfer for the two phases are given by

$$\theta'(0) = \left(1 + \frac{1}{\gamma}\right)^{-1/2} \left[-0.62755 - \frac{0.46360}{(1+\gamma)^2}\frac{1}{H} + \ldots\right], \tag{48}$$

$$\phi'(0) = \left(1 + \frac{1}{\gamma}\right)^{-1/2} \left[-0.62755 - \left(\frac{0.46360}{(1+\gamma)^2} + \frac{0.62755}{(1+\gamma)}\right)\frac{1}{H} + \ldots\right],$$

for $H \gg 1$. These curves are also plotted in Fig. 1 where excellent agreement with the full numerical solution of Eq. (46) for large values of H is observed.

Results for a vertical flat plate

The boundary layer flow induced by a constant temperature heated surface has been studied by Rees and Pop (2000) and Mohamad (2001). We take

$$S(x) = 1, \tag{49}$$

and introduce the variables

$$\psi = x^{1/2} f(x,\eta), \quad \theta = \theta(x,\eta), \quad \phi = \phi(x,\eta), \quad \eta = y/x^{1/2}. \tag{50}$$

Then Eqs. (37), (38) and (41) become

$$f' = \theta, \tag{51}$$

$$\theta'' + \frac{1}{2} f\theta' = Hx(\theta - \phi) + x\left(f'\frac{\partial\theta}{\partial x} - \theta'\frac{\partial f}{\partial x}\right), \tag{52}$$

$$\phi'' = H\gamma x(\phi - \theta), \tag{53}$$

subject to the boundary conditions

$$f = 0, \quad \theta = 1, \quad \phi = 1 \text{ at } \eta = 0, \qquad \theta, \phi \to 0, \text{ as } \eta \to \infty, \tag{54}$$

where primes denote partial derivatives with respect to η.

Equations (51)-(53) form a system of parabolic partial differential equations whose solution is nonsimilar due to the x-dependent forcing induced by the terms proportional to H. Such a nonsimilar set of equations is usually solved using a marching scheme. Beginning at the leading edge, where the system reduces to an ordinary differential system, the solution at each streamwise station is obtained in turn at increasing distances from the leading edge. Such solutions are typically supplemented by a series expansion for small values of x, and by an asymptotic analysis for large values of x. However, the present problem is not of this general nature since Eq. (53) cannot be solved at $x = 0$ while satisfying both the boundary conditions given for ϕ in (54). Thus this boundary layer has the rather unusual property of having a double-layer structure near the leading edge, rather than far from it as is often the case. This complicates considerably the numerical simulation of Eqs. (51)-(53) because it is now essential to derive the near-leading-edge solution carefully before starting the numerical work. A numerical solution which does not take this leading edge behaviour into account will exhibit numerical errors. An accurate numerical solution has been undertaken by Rees and Pop (2000) who also showed that the rates of heat transfer for the two phases are given by, as $x \to 0$,

$$\left(\frac{\partial\theta}{\partial\eta}\right)_{\eta=0} \sim b_0 - \sqrt{1+\gamma}\frac{(a_0 - \sqrt{a_0^2 + 8/\gamma})}{14.12132} x^{1/2}, \tag{55a}$$

$$\left(\frac{\partial\phi}{\partial\eta}\right)_{\eta=0} \sim -\sqrt{H\gamma}\, x^{1/2}, \tag{55b}$$

and, as $x \to \infty$,

$$\left(\frac{\partial\theta}{\partial\eta}\right)_{\eta=0} \sim \left(1 + \frac{1}{\gamma}\right)^{-1/2} [b_0 + c_0 x^{-1} \ln x + O(x^{-1})], \tag{56}$$

where $a_0 = 1.61613$, $b_0 = -0.443748$ and $c_0 = 0.0436897$. The rate of heat transfer at the solid phase $(\partial\phi/\partial\eta)_{\eta=0}$, is identical to expression (56), the leading-order difference lying at $O(x^{-1})$.

Having obtained the surface rates of heat transfer given by Eq. (55), it can be seen that these values rise indefinitely as x increases from zero; this would cause substantial inaccuracies in the numerical solution. Therefore, to integrate Eqs. (51)-(53) numerically it is convenient to introduce the new variable,

$$\xi = (Hx)^{1/2}, \tag{57}$$

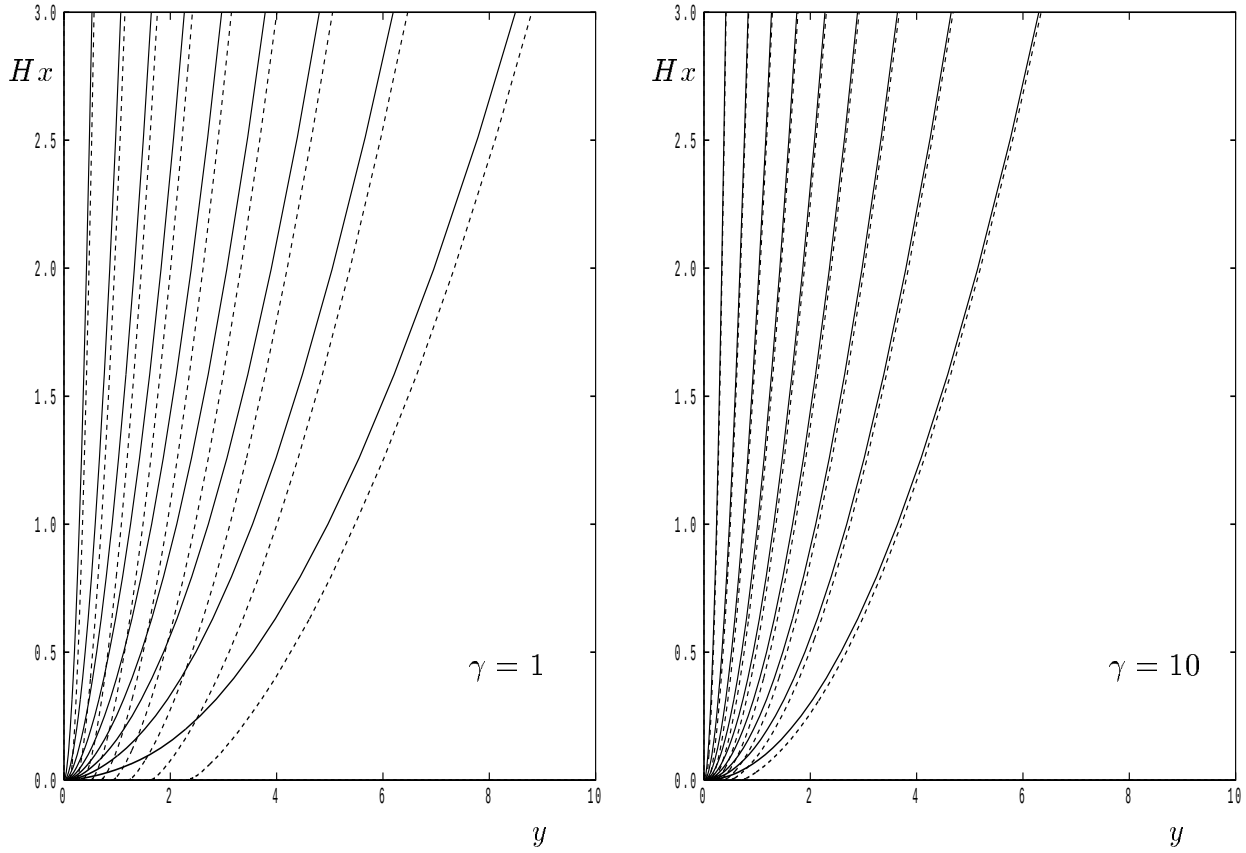

Figure 3: Isotherms for the fluid phase (solid lines) and the solid phase (dashed lines) for $\gamma = 1$ (left) and $\gamma = 10$ (right). The isotherms are reconstructed from the boundary layer solutions.

to obtain

$$f' = \theta, \tag{58}$$

$$\theta'' + \frac{1}{2} f\theta' = \xi^2(\theta - \phi) + \frac{1}{2}\xi\left(f'\frac{\partial\theta}{\partial\xi} - \theta'\frac{\partial f}{\partial\xi}\right), \tag{59}$$

$$\phi'' = \gamma\xi^2(\phi - \theta). \tag{60}$$

Equations (58)-(60) subject to the corresponding boundary conditions given in the paper by Rees and Pop (2000) have been integrated numerically using the Keller-box method along with the Newton-Raphson iteration scheme. The results obtained are summarized in Figs. 2 and 3 for the rates of heat transfer and the isotherms for both the fluid and solid phases. It is clear, from Fig. 2, that LTE is gradually attained as the distance from the leading edge, x is increased, and as H increases, since both are equivalent to an increase in ξ. Also noticeable is the fact that the solid phase surface rate of heat transfer decreases towards zero as the leading edge is approached. This is a consequence of the fact that the thermal field in the solid phase occupies a region of finite thickenss while the thermal boundary layer thickness of the fluid phase reduces to zero. This may be seen more graphically in Fig. 3 where the isotherms for both phases are illustrated for both $\gamma = 1$ and $\gamma = 10$. It is also noted that larger the value of γ, the smaller are the LTNE effects.

One interesting aspect of Fig. 3 is that the solid phase isotherms terminate on the horizontal axis at $\xi = 0$. While this might appear to be unphysical, boundary layer is unable to give information about what happens in the close neighbourhood of the origin. Therefore it was

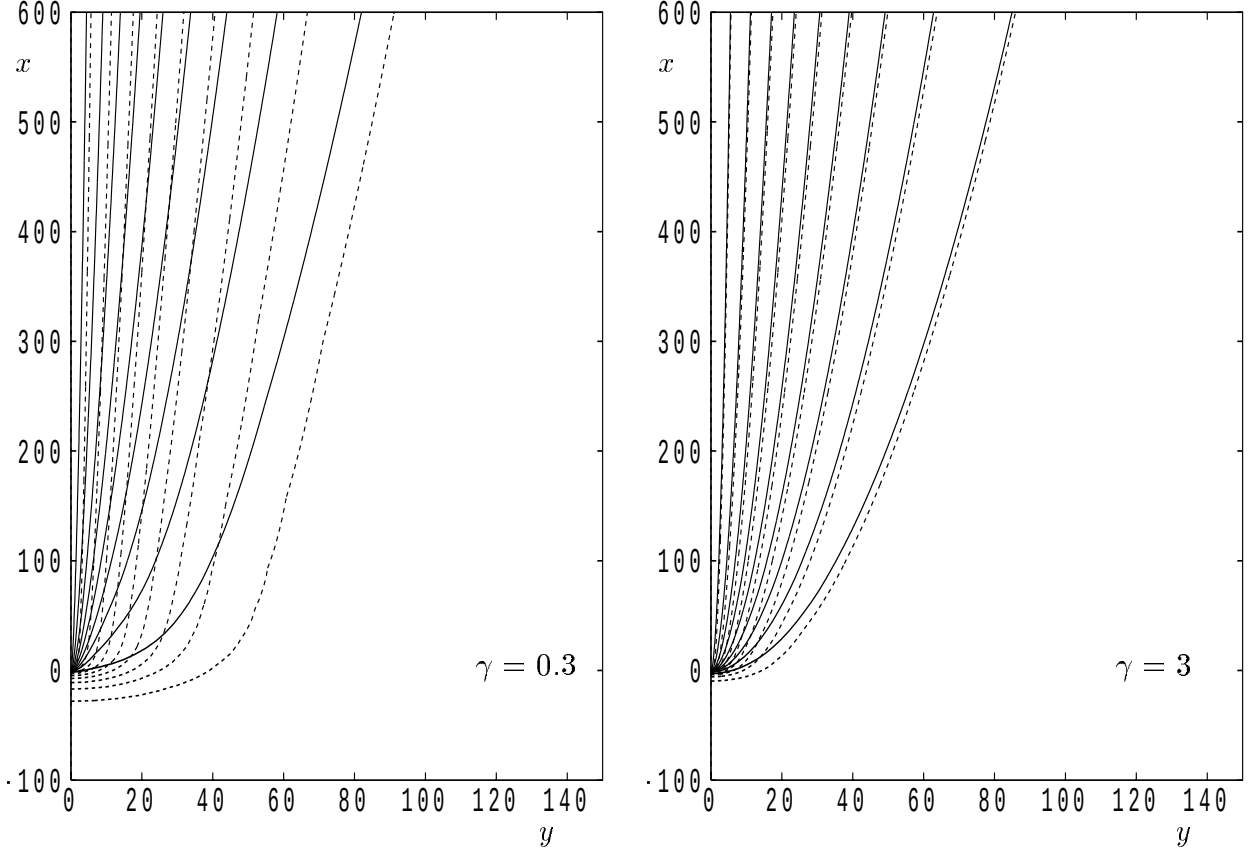

Figure 4: Isotherms for the fluid phase (solid lines) and the solid phase (dashed lines) for $\gamma = 0.3$ (left) and $\gamma = 3$ (right). The value of $\hat{h}$ is 0.01. The isotherms are obtained from solutions of the full elliptic equations.

essential to investigate that region by solving the full elliptic equations numerically; this was undertaken in Rees (2003). Fig. 4 displays such a computation for $\hat{h} = 0.01$ and for $\gamma = 0.3$ and 3. For the smaller of the two values of γ the thermal field of the solid phase extends a substantial distance below the origin, even though there is a mean upward flow due to the presence of the thermal boundary layer above. On the other hand, ther thermal field of the fluid phase is confined to $x > 0$. For the larger of the two values of γ, LTE is more nearly approximated since the two phases have almost identical thermal fields.

General comments

To our knowledge, no other papers have yet appeared which address free or mixed convective boundary layer flows when LTNE effects are strong, even though the research literature is dominated by papers for the corresponding LTE cases. The most obvious examples which remain to be considered include convection from a constant temperature (or uniform heat flux) horizontal surface, convection induced by a hot vertical cylinder, or the free convection plume. One might also extend such studies to cases where the surface temperature or heat flux is nonuniform. We think it highly likely that those LTE configurations which admit self-similarity do not retain that property when LTNE effects are strong, and that the flow near the leading edge is likely to retain the two-layer behaviour found by Rees and Pop (2000).

FORCED CONVECTION PAST A HOT CIRCULAR CYLINDER

We consider now the forced convection flow past a heated horizontal circular cylinder of radius a which is embedded in a fluid-saturated porous medium. It is assumed that the free stream velocity is U_∞ and that the temperatures of the cylinder and of the ambient fluid are T_w are T_∞. The basic equations for the steady forced convection flow past the cylinder under the condition of local thermal nonequilibrium between the fluid and the solid materials can be written in non-dimensional form as, see Rees *et al.* (2003),

$$\frac{\partial^2\psi}{\partial r^2}+\frac{1}{r}\frac{\partial\psi}{\partial r}+\frac{1}{r^2}\frac{\partial^2\psi}{\partial\alpha^2}=0, \tag{61}$$

$$\frac{1}{\mathrm{Pe}}\left[\frac{\partial^2\theta}{\partial r^2}+\frac{1}{r}\frac{\partial\theta}{\partial r}+\frac{1}{r^2}\frac{\partial^2\theta}{\partial\alpha^2}\right]=\frac{1}{r}\left[\frac{\partial\psi}{\partial\alpha}\frac{\partial\theta}{\partial r}-\frac{\partial\psi}{\partial r}\frac{\partial\theta}{\partial\alpha}\right]+H(\theta-\phi), \tag{62}$$

$$\frac{1}{\mathrm{Pe}}\left[\frac{\partial^2\phi}{\partial r^2}+\frac{1}{r}\frac{\partial\phi}{\partial r}+\frac{1}{r^2}\frac{\partial^2\phi}{\partial\alpha^2}\right]=H\gamma(\phi-\theta), \tag{63}$$

where (r,α) are the polar coordinates, ψ is the stream function which is defined as

$$u=\frac{1}{r}\frac{\partial\psi}{\partial\alpha},\quad v=-\frac{\partial\psi}{\partial r}. \tag{64}$$

Further, H is a dimensionless constant and Pe is the Péclet number given by

$$H=\frac{ah}{U_\infty(\rho c_p)_\mathrm{f}},\quad \mathrm{Pe}=\frac{U_\infty a(\rho c_p)_\mathrm{f}}{\epsilon k_\mathrm{f}}. \tag{65}$$

Equations (61)-(63) are to be solved subject to the boundary conditions

$$\psi=0,\quad \theta=\phi=1,\ \text{on } r=1 \qquad \psi\to r\sin\alpha,\quad \theta,\phi\to 0 \text{ as } r\to\infty. \tag{66}$$

The symmetry of the physical problem means that it necessary to consider only half of the physical domain, $0\le\alpha\le\pi$, with suitable symmetry conditions applied at $\alpha=0,\pi$.

For high values of the Péclet number, Pe($\gg 1$), the heat transfer problem reduces to a boundary-layer problem. However, the uniform flow past the cylinder is given by the solution of Eq. (61) and is, simply,

$$\psi=\left(r-\frac{1}{r}\right)\sin\alpha \tag{67}$$

for r large ($r\gg 1$). Substituting (67) into Eqs. (62) and (63), we obtain the following equations for the functions θ and ϕ,

$$\frac{1}{\mathrm{Pe}}\left[\frac{\partial^2\theta}{\partial r^2}+\frac{1}{r}\frac{\partial\theta}{\partial r}+\frac{1}{r^2}\frac{\partial^2\theta}{\partial\alpha^2}\right]=\left(1-\frac{1}{r^2}\right)\cos\alpha\frac{\partial\theta}{\partial r}-\left(\frac{1}{r}+\frac{1}{r^3}\right)\sin\alpha\frac{\partial\theta}{\partial\alpha}+H(\theta-\phi), \tag{68}$$

$$\frac{1}{\mathrm{Pe}}\left[\frac{\partial^2\phi}{\partial r^2}+\frac{1}{r}\frac{\partial\phi}{\partial r}+\frac{1}{r^2}\frac{\partial^2\phi}{\partial\alpha^2}\right]=H\gamma(\phi-\theta). \tag{69}$$

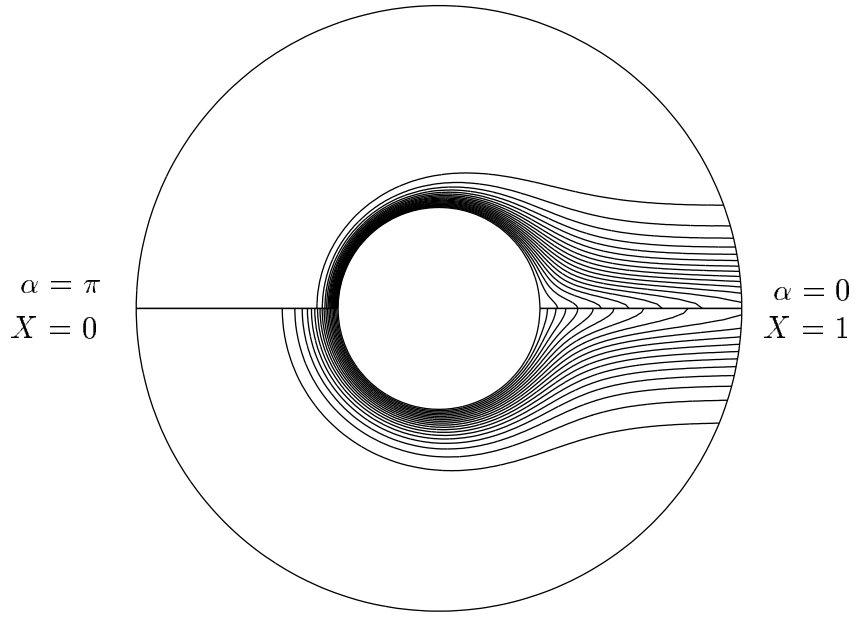

Figure 5: Computation of the temperature field for forced convection flow past a cylinder in a porous medium for $Pe = 100$, $H = 0.3$ and $\gamma = 1$. Fluid flows from left to right. The upstream (front) stagnation point corresponds to both $\alpha = \pi$ and $X = 0$. The upper half shows isotherms for the fluid phase, while the lower half corresponds to the solid phase. Isotherms are drawn at intervals of 0.05.

Pop and Yan (1998) have shown that when the fluid and solid matrix are in local thermal equilibrium the thermal field is contained within a boundary-layer which is thin compared with the radius of the cylinder whenever Pe is large. On the other hand, solving Eqs. (68) and (69) for the case of the two-equation model with Pe = 100, $H = 0.3$ and $\gamma = 1$, we can illustrate the isotherm pattern in Fig. 5, which is taken from the numerical study by Wong *et al.* (2004). This figure shows that the thermal boundary-layer thickens with distance from the upstream (front) stagnation point. Also seen is the difference in the boundary layer thicknesses between the fluid and solid phases. Having these observations in view, the following rescaled variable,

$$r = 1 + \mathrm{Pe}^{-1/2} z, \tag{70}$$

is introduced. Thus, Eqs. (68) and (69) reduce to

$$\frac{\partial^2 \theta}{\partial z^2} = 2z \cos\alpha \frac{\partial \theta}{\partial z} - 2 \sin\alpha \frac{\partial \theta}{\partial \alpha} + H(\theta - \phi), \tag{71}$$

$$\frac{\partial^2 \phi}{\partial z^2} = H\gamma(\phi - \theta), \tag{72}$$

at leading order in Pe. It proves convenient to introduce the transformation

$$\eta = z \sin\left(\frac{\alpha}{2}\right), \quad X = \cos\left(\frac{\alpha}{2}\right), \tag{73}$$

where $X = 0$ corresponds to the upstream (forward) stagnation point on the cylinder while $X = 1$ corresponds to the downstream (rear) stagnation point where the flow detaches itself from the cylinder, see Fig. 5. On using (73), Eqs. (71) and (72) become

$$\frac{\partial^2 \theta}{\partial \eta} + 2\eta \frac{\partial \theta}{\partial \eta} = 2X \frac{\partial \theta}{\partial X} + \frac{H}{1 - X^2}(\theta - \phi), \tag{74}$$

$$\frac{\partial^2 \phi}{\partial \eta^2} = \frac{H\gamma}{1 - X^2}(\phi - \theta), \tag{75}$$

and are subject to the boundary conditions

$$\theta, \phi = 1 \text{ on } \eta = 0, \qquad \theta, \phi \to 0 \text{ as } \eta \to \infty. \tag{76}$$

To this end, the local Nusselt numbers are given by

$$\mathrm{Nu_f} = -\left(\frac{\partial \theta}{\partial r}\right)_{r=1}, \quad \mathrm{Nu_s} = -\left(\frac{\partial \phi}{\partial r}\right)_{r=1}, \tag{77}$$

and, in terms of η, these may be expressed more conveniently as

$$q_\mathrm{f} = \frac{\mathrm{Nu_f}}{\mathrm{Pe}^{1/2} \sin\left(\frac{\alpha}{2}\right)} = -\left(\frac{\partial \theta}{\partial \eta}\right)_{\eta=0}, \tag{78a}$$

$$q_\mathrm{s} = \frac{\mathrm{Nu_s}}{\mathrm{Pe}^{1/2} \sin\left(\frac{\alpha}{2}\right)} = -\left(\frac{\partial \phi}{\partial \eta}\right)_{\eta=0}. \tag{78b}$$

Also, the global rates of heat transfer are given by

$$Q_\mathrm{f} = -\frac{1}{\pi}\int_0^\pi \left(\frac{\partial \theta}{\partial \eta}\right)_{\eta=0} \sin\left(\frac{\alpha}{2}\right) d\alpha = -\frac{2}{\pi}\int_0^1 \left(\frac{\partial \theta}{\partial \eta}\right)_{\eta=0} dX, \tag{79a}$$

$$Q_\mathrm{s} = -\frac{1}{\pi}\int_0^\pi \left(\frac{\partial \phi}{\partial \eta}\right)_{\eta=0} \sin\left(\frac{\alpha}{2}\right) d\alpha = -\frac{2}{\pi}\int_0^1 \left(\frac{\partial \phi}{\partial \eta}\right)_{\eta=0} dX. \tag{79b}$$

Equations (74) and (75) also form a parabolic partial differential system, which can be solved numerically by a standard finite-difference scheme except for the solution near $X = 1$, which is a singular point. At $X = 1$, Eqs. (74) and (75) reduce to the following ordinary differential equations

$$\theta'' + \frac{\gamma}{1+\gamma} 2\eta\theta' = 0, \qquad \phi'' + \frac{\gamma}{1+\gamma} 2\eta\phi' = 0, \tag{80}$$

subject to

$$\theta(0) = \phi(0) = 1, \qquad \theta, \phi \to 0 \text{ as } \eta \to \infty. \tag{81}$$

The solution of these equations is given by

$$\theta = \phi = \mathrm{erfc}\left[\left(\frac{\gamma}{1+\gamma}\right)^{1/2} \eta\right], \tag{82}$$

and therefore LTE applies at the rear stagnation point.

Equations (74) and (75), subject to the boundary conditions (76), were integrated numerically by Rees *et al.* (2003) for many values of the parameters H and γ with X in the range $0 \le X \le 1$. Fig. 6 shows the variation with X of the local rates of heat transfer q_f and q_s given by expressions (78) for $H = 0.5$, a typical case. It can be seen from Fig. 6 that large discrepancies between the rates of heat transfer of the fluid and the solid occur especially when γ is relatively small. This is to be expected because small values of γ correspond directly to cases where there is poor transfer of heat from the fluid phase to the solid phase. However, when γ is relatively large, such as for $\gamma = 100$, the temperature field of the solid phase is affected very strongly

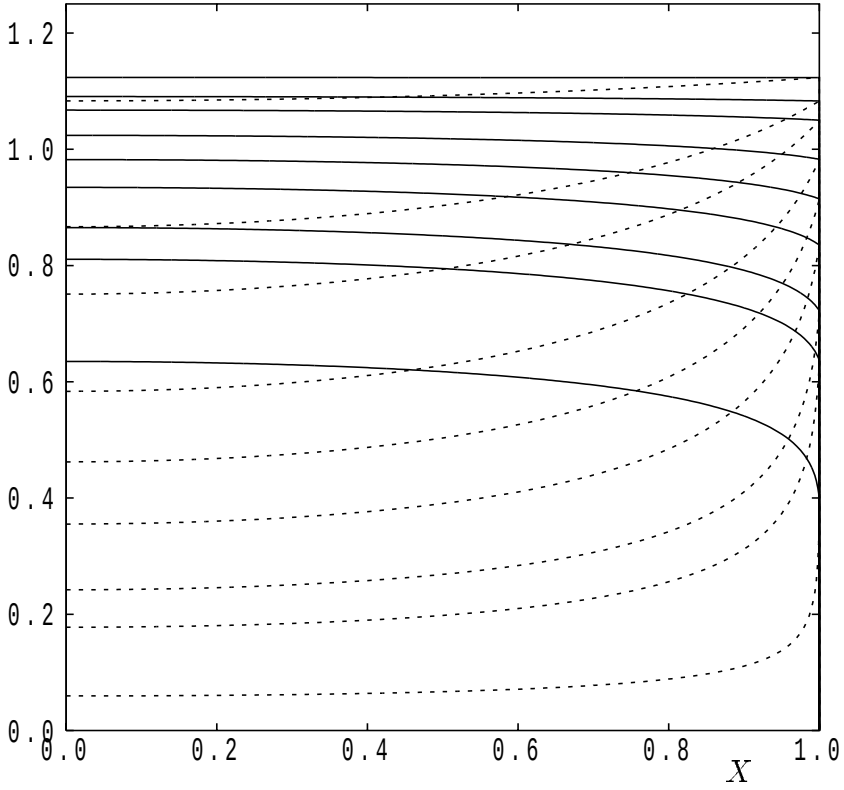

Figure 6: Variation of the local rates of heat transfer around the cylinder with X for $H = 0.5$. The continuous curves correspond to q_f and the dashed curves to q_s. Curves correspond to $\gamma = 0.01$, 0.1, 0.2, 0.5, 1.0, 2.0 5.0, 10.0 and 100.0; $\gamma = 100$ corresponds to the highest pair of curves in each subfigure.

by the temperature of the fluid phase and the two heat transfer curves are almost coincident. Although most of the cases shown in Fig. 6 exhibit strong LTNE effects, LTE is, as mentioned above, established at the rear stagnation point. This means that there are very rapid changes in the local values of both $q_{\rm f}$ and $q_{\rm s}$ near $X = 1$ when γ is small.

For other values of H, the heat transfer curves are modified in the following ways. When H takes larger values the discrepancy between $q_{\rm f}$ and $q_{\rm s}$ reduces, while LTNE effects become even stronger when H takes smaller values. We note that Rees *et al.* (2003) also provide asymptotic expressions for the rates of heat transfer for both large and small values of H. An extension of this work to forced convection past a sphere has been undertaken by Kwan (2003).

STABILITY OF FREE CONVECTION

The classical problem of stability is the Bénard problem, which consists of a constant thickness horizontal plane layer of fluid heated uniformly from below. When the two plane bounding surfaces are filled with a porous medium we have what is called either the Darcy-Bénard problem or the Horton-Rogers-Lapwood problem. A Rayleigh number is defined (see below) and it is found that the basic conduction state is stable, i.e. all possible perturbations decay, when the Rayleigh number is below a critical value. At higher values of the Rayleigh number convecting patterns form, the planform for which depend on the modelling of the porous medium, the geometry of system and the Rayleigh number, see Rees (2000, 2001).

A basic linear stability analysis was undertaken by Banu and Rees (2000) who took the two-dimensional governing equations to be

$$\frac{\partial \hat{u}}{\partial \hat{x}} + \frac{\partial \hat{v}}{\partial \hat{y}} = 0, \tag{83}$$

$$\hat{u} = -\frac{K}{\mu}\frac{\partial \hat{p}}{\partial \hat{y}}, \quad \hat{v} = -\frac{K}{\mu}\frac{\partial \hat{p}}{\partial \hat{x}} + \frac{\rho_{\rm f} g \beta K}{\mu}(T_{\rm f} - T_\infty), \tag{84, 85}$$

$$\epsilon(\rho c)_{\rm f}\frac{\partial T_{\rm f}}{\partial t} + (\rho c)_{\rm f}\underline{\hat{u}}.\nabla T_{\rm f} = \epsilon k_{\rm f}\nabla^2 T_{\rm f} + h(T_{\rm s} - T_{\rm f}), \tag{86}$$

$$(1-\epsilon)(\rho c)_{\rm s}\frac{\partial T_{\rm s}}{\partial t} = (1-\epsilon)k_{\rm s}\nabla^2 T_{\rm s} - h(T_{\rm s} - T_{\rm f}). \tag{87}$$

where circumflexes denote dimensional quantities. Equations (83) to (87) may now be nondimensionalised using the transformations,

$$(\hat{x}, \hat{y}) = d(x, y), \qquad (\hat{u}, \hat{v}) = \frac{\epsilon k_{\rm f}}{(\rho c)_{\rm f} d}(u, v), \qquad \hat{p} = \frac{k_{\rm f}\mu}{(\rho c)_{\rm f} K}p, \tag{88a, b, c}$$

$$T_{\rm f} = (T_{\rm l} - T_{\rm u})\theta + T_{\rm u}, \qquad T_{\rm s} = (T_{\rm l} - T_{\rm u})\phi + T_{\rm u}, \tag{88d, e}$$

$$\hat{t} = \frac{(\rho c)_{\rm f}}{k_{\rm f}}d^2 t, \tag{88f}$$

and by introducing the streamfunction, ψ, according to $u = -\psi_y$ and $v = \psi_x$. Equations (83)-(87) become

$$\psi_{xx} + \psi_{yy} = R\theta_x, \tag{89a}$$

$$\theta_t - \psi_y\theta_x + \psi_x\theta_y = \theta_{xx} + \theta_{yy} + H(\phi - \theta), \tag{89b}$$

$$\alpha\phi_t = \phi_{xx} + \phi_{yy} + \gamma H(\theta - \phi), \tag{89c}$$

where θ and ϕ are the respective temperatures of the fluid and solid phases. The four governing parameters,

$$R = \frac{\rho_{\rm f} g \beta (T_{\rm l} - T_{\rm u}) K d}{\epsilon \mu \kappa_{\rm f}}, \quad \gamma = \frac{\epsilon k_{\rm f}}{(1-\epsilon)k_{\rm s}}, \quad H = \frac{h d^2}{\epsilon k_{\rm f}}, \qquad \text{and} \quad \alpha = \frac{(\rho c)_{\rm s}}{(\rho c)_{\rm f}}\frac{k_{\rm f}}{k_{\rm s}}, \tag{90}$$

are the Darcy–Rayleigh number based on the fluid properties, a porosity–modified conductivity ratio, a scaled inter–phase heat transfer coefficient, and a diffusivity ratio.

The basic conducting state which we analyse for stability is given by $\psi = 0, \qquad \theta = \phi = 1 - y$. We perturb eqs. (89) about this basic solution by setting

$$\psi = \Psi, \qquad \theta = 1 - y + \Theta, \qquad \phi = 1 - y + \Phi \tag{91}$$

and linearising. Hence we obtain,

$$\Psi_{xx} + \Psi_{yy} = R\Theta_x, \tag{92a}$$

$$\Theta_t = \Theta_{xx} + \Theta_{yy} + \Psi_x + H(\Phi - \Theta), \tag{92b}$$

$$\alpha\Phi_t = \Phi_{xx} + \Phi_{yy} + \gamma H(\Theta - \Phi), \tag{92c}$$

which admit solutions of the form,

$$\Psi = A_1 \sin \pi y \cos mx, \qquad \Theta = A_2 \sin \pi y \sin mx, \qquad \Phi = A_3 \sin \pi y \sin mx, \tag{93}$$

where m is the wavenumber and where A_1, A_2 and A_3 are constants which satisfy a homogeneous system of three linear equations forming an eigenvalue problem for R in terms of H, γ and m. We obtain the following expression for R,

$$R = \frac{(\pi^2 + m^2)^2}{m^2} \Big[\frac{(\pi^2 + m^2) + H(1+\gamma)}{(\pi^2 + m^2 + \gamma H)} \Big] \tag{94}$$

After minimising R with respect to m, we obtain the critical values of R_c and m_c shown in Figs. 7 and 8.

Fig. 7 shows that R_c rises from $4\pi^2$ when H is small to a value given by $R_c = 4\pi^2(1+\gamma)/\gamma$ when H is large. It should be noted that R is the Darcy-Rayleigh number based on the properties of the fluid while $R\gamma/(1+\gamma)$ is the Darcy-Rayleigh based on the mean properties of the porous medium.

For large values of H, we therefore recover the LTE result namely that $R_c\gamma/(1+\gamma) = 4\pi^2$ with the wavenumber $m_c = \pi$. In this case the temperature fields are almost identical. On the other hand, when H is small, the perturbation in the solid phase temperature is much smaller than that in the fluid phase, and therefore the porous medium acts in a way which is independent of the solid phase. Therefore we obtain the limiting behaviour that $R_c = 4\pi^2$ with $m_c = \pi$. Between these two extremes the critical Rayleigh number increases with H, while m_c rises to a maximum and decays back to π, as shown in Fig. 8. Banu and Rees (2000) also determine detailed asymptotic representations for R_c and m_c in the large-H and small-H limits, and in the large-γ and small-γ limits.

The above analysis merely gives the criterion for the onset of convection. Weakly nonlinear theory then gives an indication of the planform the ensuing convection takes. The ansatz given in (93) yields a two-dimensional roll pattern, and more complicated patterns may be obtained by superimposing rolls of other orientations. For the classical Darcy-Bénard convection problem using the one-temperature model it is a fairly straightforward, if lengthy, matter to show that rolls are favoured over other patterns such as rectangles, squares or hexagons in a horizontally unbounded layer, see Rees (2001). In unpublished work the present authors have considered such a weakly nonlinear analysis for the above two-temperature model which concludes that rolls remain the favoured pattern for all combinations of H and γ values.

An extension of the work of Banu and Rees (2000) was undertaken by Postelnicu and Rees (2003) to allow for the additional effects of the Brinkman terms in the momentum equation. These latter authors assumed stress-free boundaries since it is then possible to solve the full equations analytically. The extra parameter is now the Darcy number, and the corresponding expression for R in terms of D, H and γ is given by,

$$R = \frac{(\pi^2 + m^2)^2}{m^2} \Big[1 + D(\pi^2 + m^2) \Big] \Big[\frac{(\pi^2 + m^2) + H(1+\gamma)}{(\pi^2 + m^2 + \gamma H)} \Big]. \tag{95}$$

Detailed results are, of course, different from those of Banu and Rees (2000) but share the same qualitative characteristics.

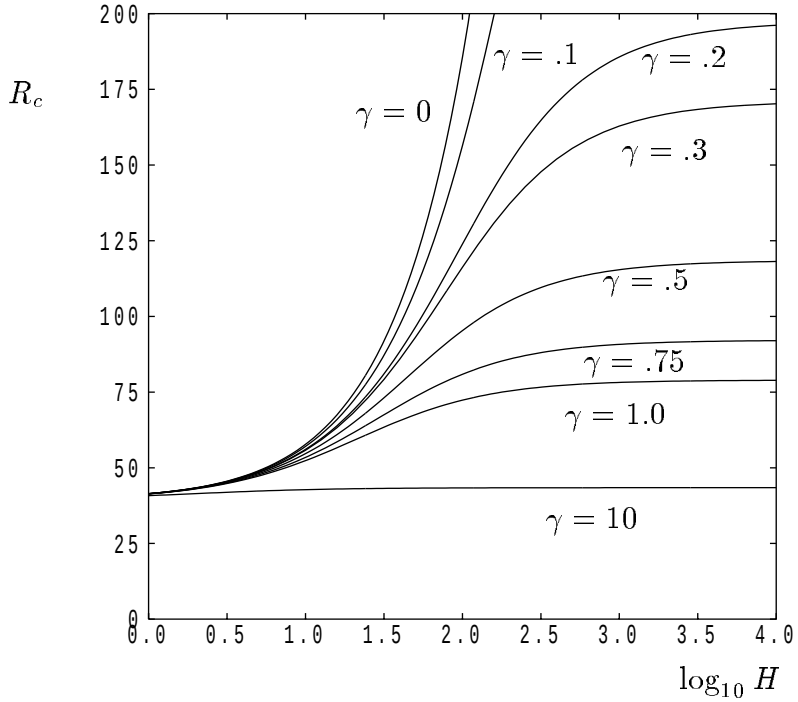

Figure 7: Variation of the critical Rayleigh number, R_c, with $\log_{10} H$ for specific values of γ.

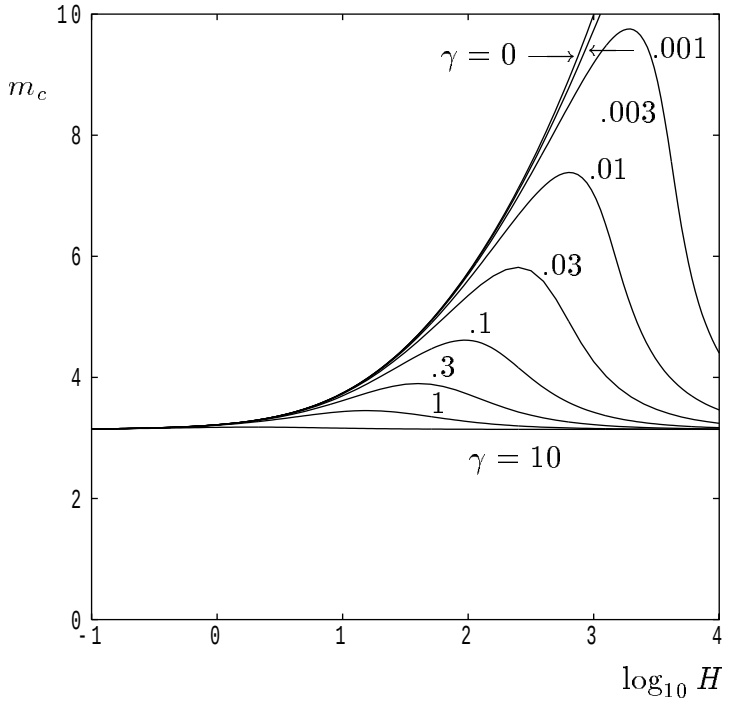

Figure 8: Variation of the critical wavenumber with $\log_{10} H$ for specific values of γ.

To date we are unaware of any computations of strongly nonlinear convection using the two-temperature model except for a very early paper by Combarnous and Bories (1974). In this work a finite difference solution was carried out for a unit aspect ratio cavity at a Rayleigh number of 200, which is well above $4\pi^2$. Comparisons where made between solutions corresponding to different values of the parameters which we denote by H and γ .

Although the following does not address the aspect of stability, there exist two papers which also consider free convection in cavities but with sidewall heating and cooling. The aim of the paper by Baytas and Pop (2002) was to describe the steady free convection in a porous two-dimensional square cavity using a the LTNE model given in Eqs. (1) and (2). The cavity is bounded by isothermal vertical walls at different temperatures and has adiabatic horizontal walls. The governing equations in terms of the non-dimensional streamfunction and temperature fields were solved numerically using the Alternating Direction Implicit (ADI) scheme. The reported results reveal, under others, that the values of the average Nusselt number for the solid phase are smaller than those for the fluid phase, respectively, because the solid phase temperature field undergoes less of a deformation from the uniform-gradient conduction state. However, these values tend asymptotically to the same values as both the modified conductivity ratio, γ, and the dimensionless scaled values of the volumetric heat transfer coefficient between the phases, H, increase. This is in qualitative agreement with the above-quoted results of Rees and Pop (1999, 2000) for the case of boundary layer flow over a vertical surface or near the lower stagnation point of a cylindrical surfacee. A similar study was carried out by Mohamad (2000) who concentrated on the validity of LTE assumption when using the Forchheimer-Brinkman extension to Darcy's law.

Finally we need to mention the numerical study of Baytas (2003) who considered LTNE effects of convection in a square cavity which is induced by internal volumetric heating within the solid phase, and with the Brinkman-Forchheimer extended Darcy law for the momentum equations. Attention was focused on the steady-state cases which arises when the Rayleigh number is not too large.

CONCLUSIONS

In this brief review we have concentrated on presenting the various two-equation models which have been proposed to account for LTNE in porous convection, and have described many recent studies including external boundary layers, free convection and stability. We have omitted both the derivation of these models, and their application to forced convective channel flows.

Although there are an increasing number of papers available in the research, there remain many topics which are, as yet, unresearched. These include the following. (i) free, mixed and forced convection plumes and other boundary layers, such as that induced by a heated vertical cylinder; (ii) the stability of thermal boundary layer flows; (iii) unsteady boundary layer flows, including those set up by a sudden change in the boundary temperature or heat flux, and those induced by time-periodic forcing; (iv) the effects on leading-edge singularities; Studies with (v) the onset of unsteady convection in porous layers heated from below; (vi) convection in horizontal cylinders; (vii) application to turbulent convection.

Notwithstanding the above paragraph, most of the research literature which either includes LTNE effects or examines its validity, assumes the simplest model given in Eqs. (1) and (2). The more complicated models which exist, such as that given by Eqs. (19) and (20), or where dispersion conductivities are included, Eqs. (17) and (18), have not yet been applied even to classical flows such as Darcy-Bénard convection and free convection boundary layer flows. However the overall aim is that an improved understanding of the fundamental convective flow processes in porous media using the LTNE model can serve to stimulate new innovations, as well as lead to improvements in the performance, reliability and costs of many existing heat transfer devices.

Acknowledgement

The second author (IP) wishes to express his cordial thanks to the Royal Society for financial support.

REFERENCES

Alazmi, B. and Vafai, K. (2000) Analysis of variants within the porous media transport models *Trans. A.S.M.E. J. Heat Transfer* **122**, 303-326.

Al-Nimr, M.A. and Abu-Hijleh, B.A. (2002) Validation of thermal equilibrium assumption in transient forced convection flow in porous channel *Transp. Porous Media* **49**, 127-138.

Al-Nimr, M.A. and Kiwan, S. (2002) Examination of the thermal equilibrium assumption in periodic forced convection in a porous channel *J. Porous Media* **5**, 35-40.

Amiri, A. and Vafai, K. (1994) Analysis of dispersion effects and non-thermal equilibrium, non-Darcian, variable porosity incompressible flow through porous media *Int. J. Heat Mass Transfer* **37**, 939-954.

Amiri, A. and Vafai, K. (1998) Transient analysis of incompressible flow through a packed bed *Int. J. Heat Mass Transfer* **41**, 4259-4279.

Banu, N. and Rees, D.A.S. (2001) The onset of Darcy-Benard convection using a thermal nonequilibrium model *Int. J. Heat Mass Transfer* **45**, 2221-2228.

Baytas, A.C. and Pop, I. (2002) Free convection in a square porous cavity using a thermal nonequilibrium model *Int. J. Thermal Sci.* **41**, 861-870.

Baytas, A.C. (2003) Thermal non-equilibrium natural convection in a square enclosure filled with a heat-generating solid phase, non-Darcy porous medium *Int. J. Energy Res.* **27**, 975-988.

Carbonell, R.G. and Whitaker, S., (1984) Heat and mass transfer in porous media. In: Fundamentals of Transport Phenomena in porous media (J. Bear and M.Y. Corapcioglu, eds), Martinus Nijhoff, Dordrecht.

Cheng, P. and C.T. Hsu, (1998) Heat conduction. In: Transport Phenomena in Porous Media (D.B. Ingham and I. Pop, eds.), Pergamon, Oxford.

Combarnous, M. and Bories, S. (1974) Modelisation de la convection naturelle au sein d'une couche poreuse horizontal l'aide d'un coefficient de transfert solide-fluide *Int. J. Heat Mass Transfer* **17**, 505-515.

Dixon, A.G. and Cresswell, D.L. (1979) Theoretical prediction of effective heat transfer parameters in packed beds *A.I.Ch.E. J.* **25**, 663-676.

Dullien, F.A.L., (1979) Porous media fluid transport and pore structure, Academic Press, New York.

Fourie, J.G. and Du Plessis, J.P. (2003a) A two-equation model for heat conduction in porous media (I. Theory) *Transp. Porous Media* **53**, 145-161.

Fourie, J.G. and Du Plessis, J.P. (2003b) A two-equation model for heat conduction in porous media (II. Application) *Transp. Porous Media* **53**, 145-161.

Kim, S.J. and Kim, D. (2001) Thermal interaction at the interface between a porous medium at an impermeable wall *Trans. A.S.M.E. J. Heat Transfer* **123**, 527-533.

Kim, S.Y. and Kuznetsov, A.V. (2003) Optimization of pin-fin heat sinks using anisotropic local thermal nonequilibrium porous model in a jet impinging channel *Num. Heat Transfer* **A44**, 771-787.

Kuwahara, F., Shirota, M. and Nakayama, A. (2001) A numerical study of interfacial convective heat transfer coefficient in two-energy model for convection in porous media *Int. J. Heat Mass Transfer* **44**, 1153-1159.

Kuznetsov, A.V., (1998) Thermal nonequilibrium forced convection in porous media. In: Transport Phenomena in Porous Media (D.B. Ingham and I. Pop, eds.), Pergamon, Oxford.

Kwan, H.Y.H., (2003) The effects of local thermal nonequilibrium on forced convection past a hot sphere embedded in a porous medium, Final year undergraduate thesis, AT26/2003, Department of Mechanical Engineering, University of Bath, Bath, UK.

Magyari, E. and Keller, B. (2002) Note on 'A two-equation analysis of convection heat transfer in porous media' by H. Y. Zhang and X. Y. Huang *Transp. Porous Media* **46**, 109-112.

Minkowycz, W.J., Haji-Sheik, A. and Vafai, K. (1999) On departure form local thermal equilibrium in porous media due to rapidly changing heat source: the Sparrow number *Int. J. Heat Mass Transfer* **42**, 3373-3385.

Mohamad, A.A. (2000) Nonequilibrium natural convection in a differentially heated cavity filled with a saturated porous matrix *Trans. A.S.M.E. J. Heat Transfer* **122**, 380-384.

Mohamad, A.A. (2001) Natural convection from a vertical plate in a saturated porous medium: nonequilibrium theory *J. Porous Media* **4**, 181-186.

Nakayama, A., Kuwahara, F., Sugiyama, M. and Xu, G. (2001) A two-energy model for conduction and convection in porous media *Int. J. Heat Mass Transfer* **44**, 4375-4379.

Nield, D.A. (1998) Effects of local thermal nonequilibrium in steady convective processes in a saturated porous medium: forced convection in a channel *J. Porous Media* **1**, 181-186.

Nield, D.A. (2002) A note on the modeling of local thermal non-equilibrium in a structured porous medium *Int. J. Heat Mass Transfer* **45**, 4367-4368.

Nield, D.A. and Bejan, A., (1999) Convection in Porous Media (2nd edition), Springer, New York.

Pop, I. and Yan, B. (1998) Forced convection flow past a cylinder and a sphere in a Darcian

fluid at large Péclet numbers *Int. Comm. Heat Mass Transfer* **25**, 261-267.

Postelnicu, A. and Rees, D.A.S. (2003) The onset of Darcy-Brinkman convection in a porous layer using a thermal nonequilibrium model - Part I: stress free boundaries *Int. J. Energy Res.* **27**, 961-973.

Quintard, M. (1998) Modelling local non-equilibrium heat transfer in porous media, Proc. 11th Int. Heat Transfer Conf., Kyong-ju, Korea, August 1998, **1**, pp. 279-285.

Quintard, M. and Whitaker, S. (1993) One and two-equation models for transient diffusion processes in two-phase systems *Adv. Heat Transfer* **23**, 369-464.

Quintard, M., Kaviany, M. and Whitaker, S. (1997) Two-medium treatment of heat transfer in porous media: numerical results for effective properties *Adv. Water Resources* **20**, 77-94.

Quintard, M. and Whitaker, S. (2000) Theoretical analysis of transport in porous media. In: Handbook of porous media (Vafai, K., ed.), Marcel Dekker, New York, pp. 1-51.

Rees, D.A.S., (2000) The stability of Darcy-Bénard convection. In: Handbook of Porous Media (K. Vafai, Ed.) pp. 521–558, Marcel Dekker, New York.

Rees, D.A.S., (2001) Stability analysis of Darcy-Bénard convection, Unpublished lecture notes from the Summer School on Porous Medium Flows, Neptun, Constanţ, Romania (25-29 June 2001).

Rees, D.A.S. (2003) Vertical free convective boundary-layer flow in a porous medium using a thermal nonequilibrium model: elliptic effects *J. Appl. Math. Phys. (Z.A.M.P.)* **54**, 437-448.

Rees, D.A.S. and Pop, I. (1999) Free convective stagnation-point flow in a porous medium using a thermal nonequilibrium model *Int. Comm. Heat Mass Transfer* **26**, 945-954.

Rees, D.A.S. and Pop, I. (2000) Vertical free convection boundary layer flow in a porous medium using a thermal nonequilibrium model *J. Porous Media* **3**, 31-44.

Rees, D.A.S., Bassom, A.P. and Pop, I. (2003) Forced convection past a heated cylinder in a porous medium using a thermal nonequilibrium model: boundary layer analysis *Eur. J. Mech. B/Fluids* **22**, 473-486.

Schumann, T.E.W. (1929) Heat transfer; a liquid flowing through a porous prism *J. Franklin Institute* **208**, 405-416.

Vafai, K. and Amiri, A., (1998) Non-Darcy effects in confined forced convective flows. In: Transport Phenomena in Porous Media (D.B. Ingham and I. Pop, eds.) pp. 313-329, Pergamon, Oxford.

Wakao, N. and Kaguei, S., (1982) Heat and mass transfer in packed beds, Gordon and Breach, New York.

Wakao N., Kaguei, S. and Funazkri, T. (1979) Effect of fluid dispersion coefficients on particle-to-fluid heat transfer coefficients in packed beds *Chem. Eng. Sci.* **34**, 325-336.

Whitaker, S., (1999) The method of Volume Averaging. Volume 13 of Theory and Applications of Transport in Porous Media (J. Bear, series ed.), Kluwer, Dordrecht.

Wong, W.S., Rees, D.A.S. and Pop, I. (2004) Forced convection past a heated cylinder in a porous medium using a thermal nonequilibrium model: finite Péclet number effects *Int. J. Thermal Sci.* **43**, 213-220.

Zhang, H.Y. and Huang, X.Y. (2001) A two-equation analysis of convection in porous media *Transp. Porous Media* **44**, 305-324.

Zhang, H.Y. and Huang, X.Y. (2002) Reply to the note by E. Magyari and B. Keller *Transp. Porous Media* **46**, 113-115.